Analysis and Simple Circuit Design of Double Differential EMG Active Electrode

Federico Nicolás Guerrero, *Student Member, IEEE*, Enrique Mario Spinelli, and Marcelo Alejandro Haberman

***Abstract*—In this paper we present an analysis of the voltage amplifier needed for double differential (DD) sEMG measurements and a novel, very simple circuit for implementing DD active electrodes. The three-input amplifier that standalone DD active electrodes require is inherently different from a differential amplifier, and general knowledge about its design is scarce in the literature. First, the figures of merit of the amplifier are defined through a decomposition of its input signal into three orthogonal modes. This analysis reveals a mode containing EMG crosstalk components that the DD electrode should reject. Then, the effect of finite input impedance is analyzed. Because there are three terminals, minimum bounds for interference rejection ratios due to electrode and input impedance unbalances with two degrees of freedom are obtained. Finally, a novel circuit design is presented, including only a quadruple operational amplifier and a few passive components. This design is nearly as simple as the branched electrode and much simpler than the three instrumentation amplifier design, while providing robust EMG crosstalk rejection and better input impedance using unity gain buffers for each electrode input. The interference rejection limits of this input stage are analyzed. An easily replicable implementation of the proposed circuit is described, together with a parameter design guideline to adjust it to specific needs. The electrode is compared with the established alternatives, and sample sEMG signals are obtained, acquired on different body locations with dry contacts, successfully rejecting interference sources.**

***Index Terms*—Active electrodes, biomedical sensors, double differential electrodes, dry electrodes, surface electromyography.**

I. Introduction

SURFACE electromyography (sEMG) allows to acquire information about muscle activity in a non-invasive way, only requiring the placement of electrodes on the skin to measure EMG signals.

A desirable property of the sEMG signal picked up by an electrode is for it to be free of crosstalk, i.e., it should correspond to muscles directly under the electrodes with no components from the activity of other muscles. Crosstalk components can be attenuated varying the number of contacts and geometry of the electrodes [1], [2]. Several topologies of increasing complexity have been proposed, among which the so-called Linear Double Differential, or just Double Differential topology (DD) has shown to achieve good selectivity while maintaining a relatively low complexity [3]–[5]. This electrode is used in research and incorporated in commercial equipments (Ottobock 13E200, Delsys DE-3.1).

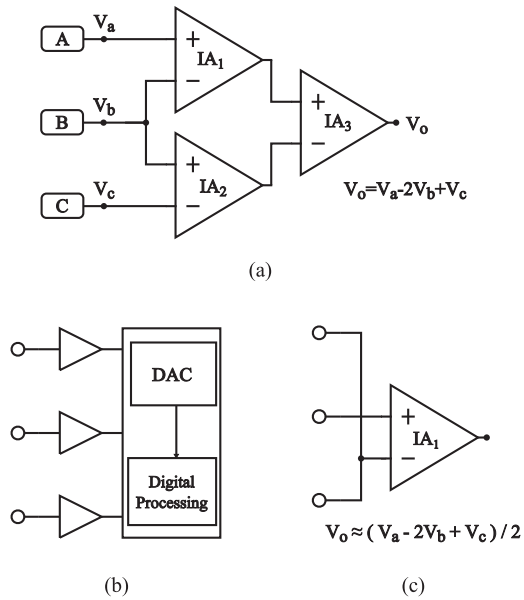

Fig. 1. Implementations alternatives found in the literature to measure the double differential (DD) signal. (a) Using three instrumentation amplifiers [2], [6]. (b) Digital processing of acquired monopolar signals [7]. (c) Approximation obtained with the branched electrode [8].

The DD topology is composed of three in-line electrodes with potentials V_{a}, V_{b} and V_{c} as depicted in Fig. 1(a). The output of the electrode, V_{o}, is the difference of the difference between two pairs of electrodes as given by the following equation:

$$V_{\mathrm{o}} = (V_{\mathrm{a}} - V_{\mathrm{b}}) - (V_{\mathrm{b}} - V_{\mathrm{c}}) = V_{\mathrm{a}} - 2V_{\mathrm{b}} + V_{\mathrm{c}}. \quad (1)$$

For many applications, especially those requiring frequent use such as rehabilitation devices, brain-computer interfaces (BCIs) or wearable biomedical sensors, it is also desirable that the electrodes are of simple placement, comfortable to wear and of low maintenance cost. This is best achieved when gel application is not needed and the electrode has no removable parts, requirements best fulfilled by pasteless or "dry" electrodes [9], [10]. Particularly for low-crosstalk configurations that bring the

Manuscript received April 30, 2015; revised July 12, 2015; accepted October 14, 2015. This work was supported in part by La Plata National University (UNLP), La Plata, Buenos Aires, Argentina, under projects PPID I-003 and PPID I-167, and in part by the National Agency for Scientific and Technological Promotion, Argentina, under project PICT-2012/0037. This paper was recommended by Associate Editor S. Leonhardt.

The authors are with the Institute of Industrial Electronics, Control and Instrumentation (LEICI), UNLP and CONICET, CC91 (1900) La Plata, Buenos Aires, Argentina, and also with the National Scientific and Technical Research Council (CONICET), Sarmiento 440, Buenos Aires, Argentina (e-mail: federico.guerrero@ing.unlp.edu.ar.).

Color versions of one or more of the figures in this paper are available online at http://ieeexplore.ieee.org.

Digital Object Identifier 10.1109/TBCAS.2015.2492944

contact plates closer together, the applied gel can protrude from under the electrode and cause a short-circuit, making pasteless electrodes preferable for these applications [11].

Dry electrodes, however, present a higher contact impedance than the wet kind [12], which makes them more susceptible to electromagnetic interference (EMI) through effects thoroughly analyzed in the literature [13], [14]. Therefore, they require a buffering stage on the electrode itself, becoming "active" electrodes. Active electrodes ideally present very high input impedance and low output impedance, resulting in acquisition systems very robust to power line interference and high electrode-skin impedance values [15]. Electrodes should also have low mass to avoid movement artifacts [16] which encourages low complexity.

One way to acquire the DD output is to digitally process signals from bipolar or monopolar channels [7] as shown in Fig. 1(b). This is usually done with EMG electrode arrays because different signal combinations are of interest. But for fixed geometry standalone electrodes it would overly increase the complexity of the system. It is also possible to acquire the EMG DD signal with only one instrumentation amplifier (IA), or even simpler implementations as seen in [17], using the "branched electrode" configuration of Fig. 1(c). This solution is very simple, but its output is equal to that of the DD only if electrode-skin impedances are perfectly balanced [8], which is very difficult to ensure. A better analog solution that always delivers the DD signal, is the three IA circuit shown in Fig. 1(a). However, this increases the component count and supply current, and it has an unbalanced input impedance that degrades the CMRR.

Designs of front-ends for measurement of the DD signal are generally presented as accessory to works about EMG signal analysis. The first examples were related to the estimation of muscle fiber conduction velocity as found in [18] and papers therein cited. These and later implementation are combinations of individual differential amplifiers, or some form of the described alternatives from Fig. 1. To the best of the authors' knowledge no other implementation of standalone sEMG DD active electrodes has been proposed in the literature. What is more, even though the properties of the DD electrode as an EMG signal transducer are thoroughly analyzed (e.g., [19], [20]), little effort has been devoted to the analysis of the three-input amplifier it requires. This circuit is obviously different from a traditional two-input differential amplifier, and a suitable analysis must be conducted in order to define the interference rejection properties of interest in EMG measurements.

In this paper we present an analysis of the DD amplifier with an emphasis on interference rejection, revealing a crosstalk interference mode, and we propose a DD active electrode implementation that is nearly as simple as the branched electrode while it verifies (1) independently of electrode-skin impedances. It can be implemented with just a quadruple operational amplifier (OA) and a few passive components, and is well suited for building low-cost compact dry active electrodes.

II. Double Differential Voltage Amplifier

A. Figures of Merit

The traditional decomposition into differential and common mode signals that is useful for two-terminal ports cannot be directly applied to a DD voltage amplifier. However, this concept can be extended by finding a transformation of the three input signals into three signal modes suitable for analyzing EMG measurements.

Two of these modes arise naturally from the characteristics of the intended EMG measurements, and are analogous to the traditional differential and common modes. One is the signal of interest given by (1), which defines a "Double Differential Mode" (DDM). The other accounts for most of the EMI interference signal. Because the body is considered equipotential in a simplified EMI model [14], this interference voltage is equal over the three input nodes. Hence this mode can be defined as the common mode (CM) signal $V_{\mathrm{CM}} = (V_{\mathrm{a}} + V_{\mathrm{b}} + V_{\mathrm{c}})/3$.

It is convenient to define the third mode as a projection orthogonal to the DDM and CM so its effect is decoupled from the signal of interest and the EMI. Hence, the third mode was defined as $V_{\mathrm{SDM}} = V_{\mathrm{a}} - V_{\mathrm{c}}$, where SDM stands for "Simple Differential Mode" in order to differentiate it from the differential mode of a two-port circuit. The whole decomposition can be represented by the following equation:

$$\begin{bmatrix} V_{\mathrm{DDM}} \\ V_{\mathrm{CM}} \\ V_{\mathrm{SDM}} \end{bmatrix} = \begin{bmatrix} 1 & -2 & 1 \\ \frac{1}{3} & \frac{1}{3} & \frac{1}{3} \\ 1 & 0 & -1 \end{bmatrix} \begin{bmatrix} V_{\mathrm{a}} \\ V_{\mathrm{b}} \\ V_{\mathrm{c}} \end{bmatrix}. \tag{2}$$

The contribution of each mode to the output can be represented using appropriate transfer functions defined as follows:

$$\begin{aligned} V_{\mathrm{o}} &= G_{\mathrm{DD}} V_{\mathrm{DDM}} + G_{\mathrm{C}} V_{\mathrm{CM}} + G_{\mathrm{SD}} V_{\mathrm{SDM}} \\ &= G_{\mathrm{DD}} \left(V_{\mathrm{DDM}} + \frac{G_{\mathrm{C}}}{G_{\mathrm{DD}}} V_{\mathrm{CM}} + \frac{G_{\mathrm{SD}}}{G_{\mathrm{DD}}} V_{\mathrm{SDM}} \right). \end{aligned} \tag{3}$$

The SDM does not contain significant EMI interference signals because EMI is equally present at all input nodes, and it neither contains the signal of interest. So, the common mode rejection ratio for a DD amplifier can be defined simply as $\mathrm{CMRR} = G_{\mathrm{DD}}/G_{\mathrm{C}}$.

However, the SDM does include a bipolar EMG signal, which contains crosstalk components that the DD electrode is meant to reject. Consequently, the ratio $G_{\mathrm{DD}}/G_{\mathrm{SD}}$ from (3) can be defined as a figure of merit. Because the SDM and DDM are both EMG signals of the same order of magnitude, the rejection coefficient does not need to be as high as the CMRR. It should also be noted that unlike the CM, which main interference components are at the line frequency and its harmonics, SDM interference has the spectral distribution of the EMG signal.

B. Finite Input Impedance

Dry electrodes present a particular challenge because their impedance has a high magnitude, with unpredictable variability between electrodes. Because the amplifier input has a finite impedance, this variability produces a non-zero CM to DDM gain that detriments the CMRR. This effect is clearly quantified

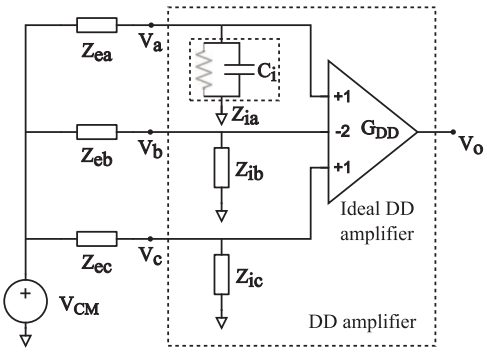

Fig. 2. Circuit representation of a double differential measurement with a common mode voltage applied. Electrode impedances are modeled by $Z_{\mathrm{ea,eb,ec}}$ and the input impedance of each terminal of the amplifier by $Z_{\mathrm{ia,ie,ic}}$.

for a differential measurement setup, through the "potential divider effect" as shown in [13]. But as the DD amplifier has three inputs, impedance unbalance has two degrees of freedom to consider. The circuit of Fig. 2 allows to analyze this effect for different cases.

For electrode impedance unbalance, the electrodes were assigned impedances $Z_{\mathrm{ea}} = Z_{\mathrm{e}} - \Delta_{\mathrm{ea}}$, $Z_{\mathrm{eb}} = Z_{\mathrm{e}}$ and $Z_{\mathrm{ec}} = Z_{\mathrm{e}} - \Delta_{\mathrm{ec}}$, and each amplifier input was considered to have the same common mode impedance, of value Z_{i}. Then, the CM to DDM gain $G_{C,Z_{\mathrm{e}}}$ can be found as the ratio $V_{\mathrm{DDM}}/V_{\mathrm{CM}}$, yielding

$$G_{C,Z_{\mathrm{e}}} = G_{\mathrm{DD}} Z_{\mathrm{i}} \frac{(\Delta_{\mathrm{ea}} + \Delta_{\mathrm{ec}})(Z_{\mathrm{i}} + Z_{\mathrm{e}}) - 2\Delta_{\mathrm{ea}}\Delta_{\mathrm{ec}}}{(Z_{\mathrm{i}} + Z_{\mathrm{e}} - \Delta_{\mathrm{ea}})(Z_{\mathrm{i}} + Z_{\mathrm{e}} - \Delta_{\mathrm{ec}})(Z_{\mathrm{i}} + Z_{\mathrm{e}})}.$$

A good approximation of this equation can be obtained when the magnitude of Z_{e} is smaller than around 10% of the magnitude of Z_{i}

$$G_{C,Z_{\mathrm{e}}} \approx G_{\mathrm{DD}} \left(\frac{\Delta_{\mathrm{ea}} + \Delta_{\mathrm{ec}}}{Z_{\mathrm{i}}} - \frac{2\Delta_{\mathrm{ea}}\Delta_{\mathrm{ec}}}{Z_{\mathrm{i}}^2} \right). \tag{4}$$

Equation (4) shows that the symmetry of the unbalance is important. If $\Delta_{\mathrm{ea}} = -\Delta_{\mathrm{ec}}$ the first term is 0 and $G_{C,Z_{\mathrm{e}}} = -2G_{\mathrm{DD}}(\Delta_{\mathrm{e}}/Z_{\mathrm{i}})^2$, but when Z_{ea} and Z_{eb} are symmetrically unbalanced with respect to Z_{eb}, i.e., $\Delta_{\mathrm{ea}} = \Delta_{\mathrm{ec}} = \Delta_{\mathrm{e}}$, the first term is higher and the second term is generally negligible because it is divided by Z_{i}^2. Thus an upper bound for $G_{C,Z_{\mathrm{e}}}$ is obtained, and it can be further expressed as a minimum rejection ratio

$$(\mathrm{CMRR}_{Z_{\mathrm{e}}})_{\min} = \frac{Z_{\mathrm{i}}}{2\Delta_{\mathrm{e}}}. \tag{5}$$

A similar effect is produced when input impedances of the amplifier are unbalanced. In this case input impedances can be assigned values $Z_{\mathrm{ia}} = Z_{\mathrm{i}} + \Delta_{\mathrm{ia}}$, $Z_{\mathrm{ib}} = Z_{\mathrm{i}}$, and $Z_{\mathrm{ic}} = Z_{\mathrm{i}} + \Delta_{\mathrm{ic}}$. Given equal electrode impedances Z_{e} and again for a worst-case

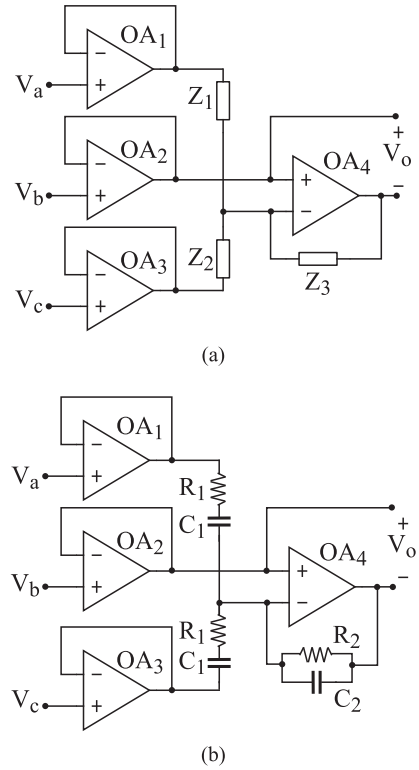

Fig. 3. (a) Proposed DD front-end for active electrodes. Each input node has an individual buffer to avoid CMRR degradation, and the output channel is differential in order to match the differential input of high resolution ADCs and maintain a high CMRR. (b) Proposed DD front-end with gain and bandwidth limitation.

symmetric unbalance when $\Delta_{\mathrm{ia}} = \Delta_{\mathrm{ic}} = \Delta_{\mathrm{i}}$, the rejection ratio due to input impedance unbalance results

$$(\mathrm{CMRR}_{Z_{\mathrm{i}}})_{\min} = \frac{Z_{\mathrm{i}}^2}{2\Delta_{\mathrm{i}} Z_{\mathrm{e}}}. \tag{6}$$

III. Proposed Circuit

The proposed circuit is depicted in Fig. 3(a). It allows to measure the DD signal in a simple way, using only a quadruple operational amplifier integrated circuit; this is less complex and power-consuming than using three instrumentation amplifiers.

The differential output results

$$V_{\mathrm{o}} = V_{\mathrm{a}} \frac{Z_3}{Z_1} - V_{\mathrm{b}} \frac{Z_3}{Z_1 || Z_2} + V_{\mathrm{c}} \frac{Z_3}{Z_2}. \tag{7}$$

Which for $Z_1 = Z_2$ yields

$$V_{\mathrm{o}} = (V_{\mathrm{a}} - 2V_{\mathrm{b}} + V_{\mathrm{c}}) \frac{Z_3}{Z_1} = V_{\mathrm{DDM}} \frac{Z_3}{Z_1}. \tag{8}$$

A. Design

Three OAs act as buffers to provide high input impedance. The fourth OA and the passive network perform the sum and difference needed for the DD output. The output presents low impedance and is differential, which is convenient because it

matches to current differential input high resolution sigma-delta ADCs, and agrees with modern instrumentation trends which are towards fully-differential (FD) circuits [21]–[23].

FD circuits have higher dynamic ranges than their single-ended (SE) counterparts thus exploiting the available power supply voltage, which is very important for portable, single supply, low voltage systems. A FD circuit that maintains no connections to ground, such as the proposed circuit, has an ideally infinite CMRR independent from component imbalances [24]. It must be noted however that FD circuits need two exclusive wires to propagate the output signal, demanding an extra wire from the active electrode to the main board in comparison with single-ended circuits.

The values given to impedances Z_{1-3} allow to configure the amplifier's transfer function. If given purely resistive values, $Z_1 = Z_2 = R_1$ and $Z_3 = R_2$, the output results $V_\mathrm{o} = V_\mathrm{DDM}(R_2/R_1)$. It is possible to assign impedances to the circuit of Fig. 3(a) to provide gain and bandwidth limitation at the front-end, leading to the circuit of Fig. 3(b). This circuit has the following band-pass transfer function:

$$V_\mathrm{o} = V_\mathrm{DDM}\frac{(\frac{R_2}{R_1})s\tau_1}{(1+s\tau_1)(1+s\tau_2)}. \tag{9}$$

Where $\tau_1 = R_1C_1$ and $\tau_2 = R_2C_2$. The middle band gain is $A_0 = R_2/R_1$, the lower cut-off frequency $f_\mathrm{l} = (2\pi\tau_1)^{-1}$ and the upper cut-off frequency $f_\mathrm{h} = (2\pi\tau_2)^{-1}$.

B. Interference Rejection

An acceptable CMRR for EMG measurements is in the range of 100–120 dB [2]. A driven right leg circuit usually provides an attenuation of at least 30–40 dB of the common mode interference, effectively incrementing the CMRR by that amount [25], [14]. Hence, a reasonable rejection value range for the measurement front end is 70–90 dB.

The CMRR of the proposed electrode can be calculated according to (3). $G_\mathrm{DD} = Z_3/Z_1$ is readily available from (8) and G_C can be calculated applying a common input V_CM to all nodes. Disregarding second order effects, the CMRR results

$$\mathrm{CMRR} = \left(\frac{1}{\mathrm{CMRR}_\mathrm{OA4}} + \frac{1}{A_\mathrm{OA4}}\right)^{-1}. \tag{10}$$

Where $\mathrm{CMRR}_\mathrm{OA4}$ and A_OA4 are the CMRR and open loop gain of the operational amplifier OA4 from Fig. 3(a). Hence an OA with both parameters remaining in a range not below 80–100 dB within the frequencies of interest should be selected to comply with the 70–90 dB objective.

The other source of CMRR degradation is the finite input impedance of the circuit, as described in Section II. The proposed design has OAs in buffer configuration for every input, which is an accepted solution in the literature [2], [26] that achieves very high impedance using low cost monolithic components.

The CMRR that this approach is able to provide was determined using (5). A range of values for the equation variables Z_in, Z_e and Δ_e, all at 50 Hz , were chosen according to the following considerations:

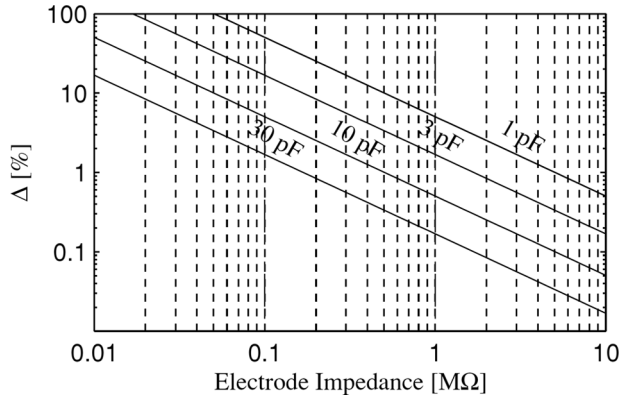

Fig. 4. 90 dB CMRR level curves parametrized by the input capacitance of the amplifier, which dominates its input impedance. They are a function of the center electrode impedance Z_e, and the symmetrical unbalance of the extreme electrodes about the center one, such that $Z_{\mathrm{a,c}} = Z_\mathrm{e}(1 + \Delta/100)$.

- Current devices, both OAs and IAs, have input impedances mostly dependent on their input capacitance, so $Z_\mathrm{in} \approx (2\times\pi\times 50\ \mathrm{Hz}\times C_\mathrm{i})^{-1}$. Usual values for C_i range from 2 pF to 30 pF (and stray capacitances from the PCB may also contribute with values in the order of a few pF).
- In [12] it is shown that different kinds of dry electrodes when first applied to unprepared skin, may have impedance values up to 1 MΩ at 50 Hz with variations across subjects or locations of up to 100%.

Using these values, level curves of 90 dB rejection were plotted in Fig. 4 parametrized by the input capacitance of the amplifier. The curves are a function of Z_e in the horizontal axis and Δ_e as a percentage of Z_e in the vertical axis. For example, for a 1 MΩ impedance, a symmetric unbalance greater than 10% would result in excessive interference even for the best OAs.

These are very unfavorable conditions, that can however occur when small area contact plates have just been positioned, or the skin is very dry. These extreme cases can be alleviated by mild skin preparation such as rubbing the skin with tap water or waiting a few minutes for sweat to moist the area under the electrode [27].

The input impedance itself can be unbalanced and cause an undesired mode transformation. In the traditional three IA DD circuit, node B is shared between two IA inputs, so the impedance it sees is half the impedance of nodes A and C. This means that for (6), $\Delta_\mathrm{i} = Z_\mathrm{i}/2$ and

$$\mathrm{CMRR}_{Z_\mathrm{i}} = \frac{Z_\mathrm{i}^2}{2(\frac{Z_\mathrm{i}}{2})Z_\mathrm{e}} = \frac{Z_\mathrm{i}}{Z_\mathrm{e}}. \tag{11}$$

Hence, in this case the CMRR always depends on the electrode impedances mean value instead of its unbalance. For $Z_\mathrm{e} = 1\ \mathrm{M\Omega}\ @\ 50$ Hz, a fairly low 3 pF input capacitance would produce a 60 dB rejection. This situation is improved by the proposed electrode because each input node is buffered and the variation of input impedances of each buffer can be neglected.

As previously discussed, the SDM has undesired crosstalk components that can be carried over to the DDM because of circuit unbalances. The SDM to DDM gain can be calculated from (7) where ideally $Z_1 = Z_2 = \bar{Z}$. Considering departures

form those values expressed for convenience by a parameter $\delta = (Z_1 - Z_2)/(Z_1 + Z_2)$, these impedances can be written as $Z_1 = \bar{Z}(1+\delta)$ and $Z_2 = \bar{Z}(1-\delta)$, so

$$V_{\mathrm{o}} = \frac{Z_3}{\bar{Z}}\left(\frac{V_{\mathrm{a}}}{1+\delta} - \frac{2V_{\mathrm{b}}}{\bar{Z}(1-\delta)(1+\delta)} + \frac{V_{\mathrm{c}}}{1-\delta}\right).$$

That for the case $\delta \ll 1$ can be approximated as

$$\begin{aligned} V_{\mathrm{o}} &= \frac{Z_3}{\bar{Z}}\left(V_{\mathrm{a}}(1-\delta) - \frac{2}{\delta}V_{\mathrm{b}} + V_{\mathrm{c}}(1+\delta)\right) \\ &= \frac{Z_3}{\bar{Z}}((V_{\mathrm{a}} - 2V_{\mathrm{b}} + V_{\mathrm{c}} + V_{\mathrm{c}}\delta - V_{\mathrm{a}}\delta) \qquad (12) \\ &= G_{\mathrm{DD}}(V_{\mathrm{DDM}} + \delta V_{\mathrm{SDM}}) \\ \Rightarrow \frac{G_{\mathrm{DD}}}{G_{\mathrm{SD}}} &= \frac{1}{\delta} = \frac{Z_1 + Z_2}{Z_1 - Z_2}. \qquad (13) \end{aligned}$$

Equation (13) is in the form of a rejection ratio coefficient. When Z_1 and Z_2 are implemented as in Fig. 3(b), the impedance of the capacitors is dominant for low frequencies and $(G_{\mathrm{DD}}/G_{\mathrm{SD}})_{\min} = \delta C$, where δC is the tolerance of the capacitor.

This analysis can be applied to the equations developed in [8] for the branched electrode to find its output $V_{\mathrm{o,BE}}$ as a function of a DD amplifier signal modes

$$V_{\mathrm{o,BE}} = G_{\mathrm{DD}}\left(V_{\mathrm{DDM}} + \frac{Z_{\mathrm{ea}} - Z_{\mathrm{ac}}}{Z_{\mathrm{ea}} + Z_{\mathrm{ac}}}V_{\mathrm{SDM}}\right).$$

This equation shows that the branched electrode does produce the desired V_{DDM}, but with a V_{SDM} interference that may be too high because it depends on the unbalance of electrode impedances.

IV. Electrode Implementation and Auxiliary Circuits

A. Implementation Details

The proposed circuit was used to build an EMG active electrode. The quadruple OA it requires was implemented with OPA4243 from Texas Instruments. This component was selected because of its low input capacitance (2 pF), high CMRR (104 dB @ 50 Hz), relatively low noise (0.6 $\mu\mathrm{V_{rms}}$ in 10–500 Hz) and 5 V single supply operation.

Two versions were assembled: 1) A version with gain 1, setting all impedances from Fig. 3(a) as 1 kΩ resistors, and 2) The band-limited version from Fig. 3(b) with a 3 dB bandwidth from 16 Hz to 500 Hz (appropriate for sEMG according to [28]) and a mid-band gain of 10, obtained with the following component values: $R_1 = 1\ \mathrm{k\Omega}$, $R_2 = 10\ \mathrm{k\Omega}$, $C_1 = 10\ \mu\mathrm{F}$, $C_2 = 32\ \mathrm{nF}$.

The electrode contacts were implemented with standard pin header connectors. These connectors are 10 mm gold plated rods with a square transversal area of 0.64 mm sides. The rods were placed parallel to each other 10 mm apart, on the back of a single-sided PCB that held the circuit. This inter-electrode distance was found optimal for crosstalk reduction in [29].

Additional mechanic support was provided to separate the rods from the wider PCB in order to ensure good contact and

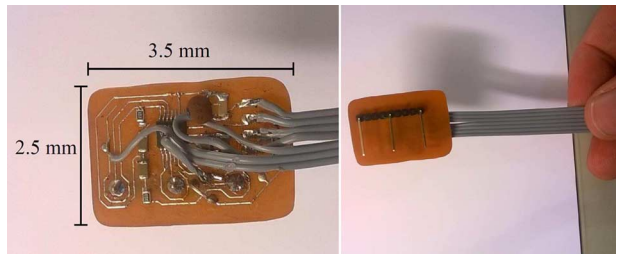

Fig. 5. Implementation of the proposed electrode with the circuit of Fig. 3(b). Four wires provide power and the differential output channel. Additional wires were included to acquire the signals from each buffer, for testing purposes.

TABLE I
Typical Performance Characteristics and Adjustment Parameters

Parameter	Value	Adjustment
CMRR	86 dB @ 50 Hz 78 dB @ 100 Hz	OA_4 open loop gain and CMRR
SDMRR	$\geq$ 40 dB	$R_{1,2}$ and $C_{1,2}$ tolerance
Power Supply Drain	$\approx 220\,\mu A$	OA selection
Input Impedance	10 GΩ || 2 pF	
Noise	1.6 $\mu\mathrm{V_{rms}}$ (17-500 Hz)	
Midband gain	20 dB	$\approx R_2/R_1$
3 dB Bandwidth	17-500 Hz	R_1C_1 , R_2C2

standard ribbon cable was used for the leads. The complete active electrode had a size of 35 mm × 25 mm × 10 mm without casing. A picture of the device is shown in Fig. 5.

Two extra wires were soldered to the outputs of OA1 and OA3, which together with the output lead from OA2 allow to acquire the signal of each contact rod individually. This modification was made for testing purposes, so as to obtain the bipolar signal from any pair of contacts in addition to the DD output.

The functioning parameters of the implemented electrode were measured and are presented in Table I. These parameters are in accordance with those recommended in the literature [2], [22], [28], and can be tailored to specific needs as indicated in the third column of Table I.

B. Auxiliary Circuits

A previously developed USB biopotential acquisition equipment based around ADS1298 from Texas Instruments was used to digitize the output of the electrode. This front-end has a differential programmable amplifier and a 24 bit Sigma-Delta converter for each acquisition channel.

The system includes a Driven Right Leg circuit [25] used to set a DC common mode voltage of 2.5 V [30] and attenuate the common-mode power-line interference 30 dB. The DRL has independent measurement and feedback electrodes with 10 mm diameter snap connectors that can either be used as dry contact plates or to attach disposable electrodes.

A second electrode was built with the three IA topology from Fig. 1(a) in order to compare the proposed circuit with a well-established alternative. AD623 IAs from Analog Devices were selected for their low input capacitance of 2 p F and single supply

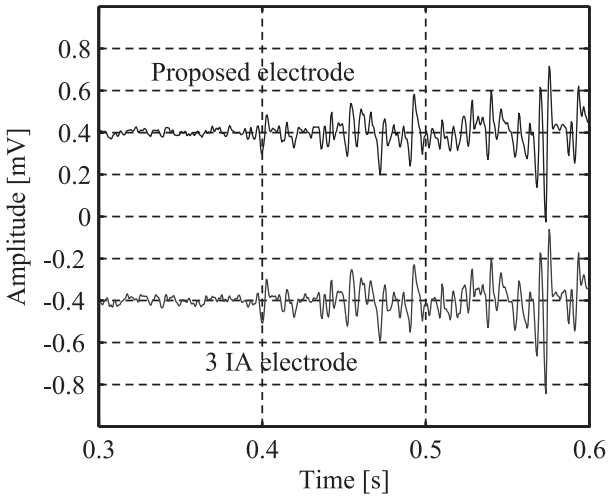

Fig. 6. sEMG signals obtained from the proposed electrode and the 3 IA electrode connected to the same contact plates. The cross-correlation of 4 s of the signals shown above was 0,994.

operation. If needed, both electrodes could operate simultaneously on the acquisition system setting a 1.75 V reference to allow a ± 0.5 V range for the AD623. All IAs were configured for a gain of 1.

V. Experimental Measurements

A set of measurements were conducted in order to verify and demonstrate the performance of the proposed electrode.

A. Verification Against the Three IA Topology

The proposed electrode was tested against the previously described 3 IA DD electrode. Both circuits were soldered to the same contact rods and their outputs simultaneously acquired with two channels of the measurement system. The unity gain version of the proposed electrode was used in this test in order to avoid differences due to component tolerances in the transfer characteristics.

This "Dual" electrode was placed over the medial bulge of the forearm of one of the authors, and held in place using adjustable elastic bands. The DRL was affixed on the palm side of the wrist using standard 3M disposable electrodes. Complete flexions of the index finger were executed. The signals were acquired with a 2000 Hz sampling rate, gain of 1, and off-line filtered with a 2nd order bandpass Butterworth filter with a 10 Hz to 600 Hz bandwidth.

The normalized cross-correlation of the two signals was calculated over a 4 s segment during muscle activation, obtaining a correlation coefficient $\rho = 0,994$. A fragment showing the onset of sEMG activity is presented in Fig. 6 for visual verification. This test allowed to verify that the proposed electrode produces the same DD output than the established alternative.

B. EMG Measurements

Next, the band-limited version of the proposed electrode was affixed over the biceps brachii muscle, and isometric contractions were executed trying to achieve maximal contraction. The resulting raw signal can be seen in Fig. 7(a). A second measurement was conducted placing the electrode over the medial

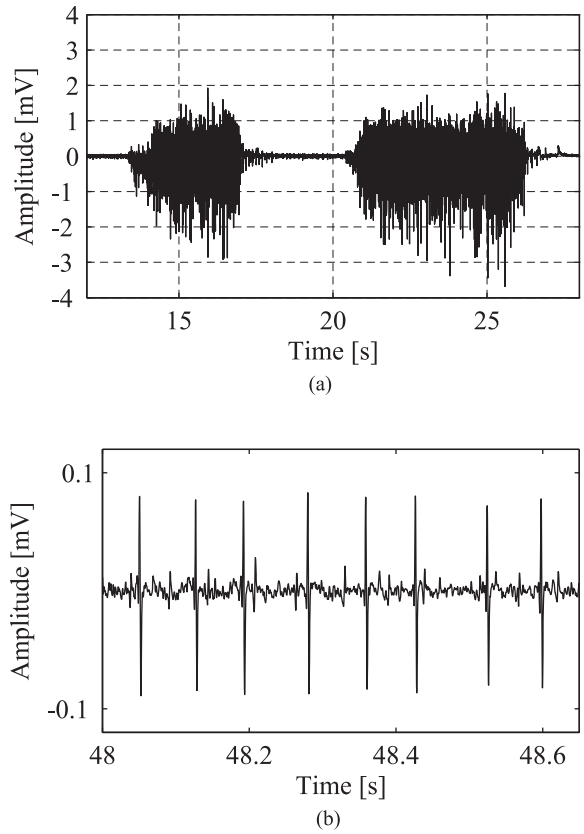

Fig. 7. sEMG recordings obtained with the presented electrode. (a) Shows a measurement of two consecutive strong isometric contractions of the biceps braccii. (b) Sample of the signal obtained from the medial bulge of the forearm when a gentle flexion of the index finger was executed.

bulge of the forearm. This position was selected because muscle activity elicited by gentle flexion of the index finger could be easily detected, as shown in Fig. 7(b). These sample recordings allow to observe signal levels with and without EMG activity, and the electrode performance measuring both high and low amplitude signals.

C. Crosstalk Rejection

A set of measurements presented in Fig. 8 were conducted in order to visualize the crosstalk rejection capabilities of the proposed electrode in a simple way. Two locations were selected where specific movements activated spatially close but sufficiently separate muscles. The additional wires of the prototype were used to simultaneously acquire the DD output of the electrode and a bipolar signal, obtained as the difference of contact rods B and C potentials with an inter-electrode distance of 10 mm. All signals were post-processed with a 100 m s moving average filter.

For Fig. 8(a) the electrode was positioned on the forearm over the finger extensor muscles, close to the elbow. A location where the extension of index finger produced the maximum amplitude was selected. The observed signals were produced by extending the index finger followed by relaxation and then extending the little finger. For Fig. 8(b) the electrode was positioned on the cheek in order to detect the contraction of the zygomaticus muscles. The observed EMG activity was elicited by

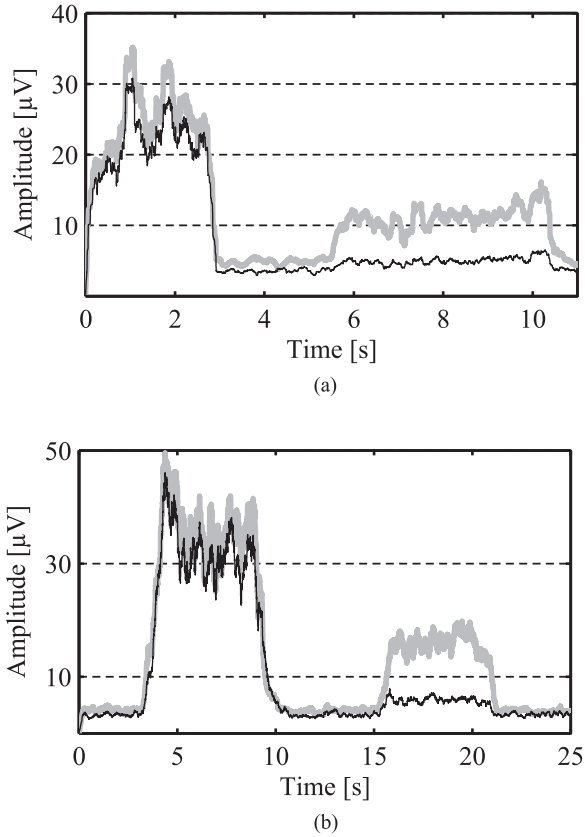

Fig. 8. Filtered sEMG DD signals (black line) obtained with the proposed electrode and bipolar signals (gray line) obtained from two contiguous contacts of the same electrode 10 mm appart. (a) was measured on the forearm by extending first the index and then the little finger, and (b) on the cheek by smiling and then clenching the jaws together.

performing a smiling expression first, and clenching the jaws together next. Both figures show the attenuation that the DD electrode produces over sEMG signals generated by muscles not directly underneath it, compared with the bipolar electrode of 10 mm inter-electrode distance formed by two rods of the DD electrode.

D. Interference Rejection

The results presented in (11) were experimentally verified. The measurement setup of Fig. 2 was implemented for this test. A 70 Hz, 1 V_{pp} sine wave was applied at V_{CM} and three sets of measurements were conducted for both electrodes. In each measurement, Z_{ea}, Z_{eb} and Z_{ec} were implemented with three resistors of equal value, and this value was varied across sets. The proposed electrode's CMRR was 81 dB and did not show significant change across measurements. The results for the three IA topology are presented in Table II. For the lowest value of 22 kΩ, the effect was not noticeable because the CMRR of the AD623 is lower. However when higher resistance values were applied, the CMRR was degraded to values close to those predicted by (11).

Next, this effect was tested with measurements on the body. Fig. 2 and Table II show that when the impedance of the electrodes is very high, the potential divider effect (proportional to ΔZ_e) and the input impedance unbalance (proportional to Z_e for the 3 IA electrode) can become the main common mode interference mechanisms. Hence, the common mode interference will be lower or equal for the proposed electrode compared with the 3 IA electrode, as the relation will be proportional to the ratio of ΔZ_e to Z_e that can be at most unity.

TABLE II
70 HZ CMRR OF THE THREE IA ELECTRODE FOR INCREASING VALUES OF SOURCE IMPEDANCE

$Z_{ea,eb,ec}$ [kΩ]	Measured value [dB]	Predicted Value (Eq. 11) [dB]
22	83.2	94.2
220	73.6	74.2
2200	51.4	54.2

In order to avoid other interference mechanisms to mask the phenomenon to be observed, a 70 Hz common mode signal was imposed on the body and measured through one of the leads of the proposed electrode. Both the proposed and the 3 IA electrodes were placed next to each other on the forearm and 5 recordings were made with varying conditions: tight and loose elastic bands, interchanging locations, and within different times of application from 10 s to 60 s. A least squares approximation of the 70 Hz signal present in every recording was performed and the rejection difference calculated. The proposed electrode had a (15 ± 4) dB better rejection over the 3 IA electrode across measurements.

VI. CONCLUSIONS

The literature supports the use of double differential sEMG electrodes for crosstalk reduction. In particular, standalone dry active electrodes have many applications and commercial devices exist. However, implementation details and general knowledge about the design of the needed amplifier seem scarce in the literature.

Hence in this paper we first set out to perform a basic analysis of the three-input DD amplifier to evaluate its functioning parameters. Then, we presented a novel circuit for a DD active electrode with very low complexity and cost, including only a quadruple operational amplifier and a few passive components, that allowed to acquire sEMG signals with dry contacts rejecting interference sources.

A. Circuit Analysis

Three signal modes that characterize the input of the amplifier were proposed: a mode carrying the signal of interest V_{DDM}, a mode accounting for EMI V_{CM}, and a third orthogonal mode V_{SDM}, that is of note because it is the bipolar EMG signal. As the purpose of the DD amplifier is to attenuate the crosstalk components found in the bipolar EMG, V_{SDM} must be rejected, meaning attention should be paid to the circuit parameters that allow this signal to reach the output.

Next, the equations that account for EMI produced by electrode and input impedance unbalances were obtained. Because there are three terminals, impedance unbalance has two degrees of freedom, and the worst-case interference occurs when node A and C impedances (either of the electrodes or the inputs)

are symmetrically unbalanced about that of node B. Approximated equations for this case allowed to obtain expressions for the minimum expected CMRR, as a function of input and electrode impedance value and unbalance. The CMRR degradation that the unbalanced input stage produces was experimentally demonstrated.

B. Proposed Active Electrode Implementation

A circuit for a double differential active electrode was presented. It was much simpler than the instrumentation-amplifier based alternative found in the literature, reducing the number of OAs needed for the design, and achieving at the same time the desired DD output independently of electrode impedance, in contrast with the branched electrode configuration. The circuit has a differential output, matching to the input of current high performance biopotential front-ends.

An implementation of the proposed circuit was described, built entirely with readily available commercial components and easily replicable. Its functioning parameters were experimentally measured and resulted in agreement with specifications found in the literature. These parameters can be adjusted to best suit different applications as shown in Table I.

The input stage was designed with a unity gain buffer for each contact plate. The limits of this stage when implemented with off-the-shelve components were investigated using the worst-case EMI electrode unbalance equation. It was concluded that for some extreme cases, mild skin preparation or waiting a few minutes would be necessary even with the best components available. If this is to be avoided a more complex input stage would be required. However, it was theoretically and experimentally shown that the implemented input has better common mode rejection compared with the three IA based topology where one contact plate feeds two input terminals. This is not to be confused with the overall common mode rejection ratio, which is not intrinsically better and depends on component selection.

The implemented device was experimentally tested, showing that this simple topology produces the same DD output than the IA based electrode in a standard biopotential measurement setup. A range of sEMG signal measurements were carried out on different locations on the body, using dry electrodes without skin preparation. High quality signals were obtained without significant EMI components and showing the crosstalk rejection properties of the electrode.

ACKNOWLEDGMENT

The authors wish to thank Texas Instruments for providing free samples of components used in this work.

REFERENCES

[1] H. Reucher, G. Rau, and J. Silny, "Spatial filtering of noninvasive multielectrode EMG: Part I-introduction to measuring technique and applications," *IEEE Trans. Biomed. Eng.*, vol. BME-34, no. 2, pp. 98–105, Feb. 1987.

[2] R. Merletti and P. Parker, *Electromyography: Physiology, Engineering, and Non-Invasive Applications*. Hoboken, NJ, USA: Wiley, 2004.

[3] Y. Chen, C. A. Laszlo, and C. Hershler, "A quantitative evaluation of methods for recording surface electromyogram," in *Proc. Annu. Int. Conf. IEEE Eng. Med. Biol. Soc.*, 1993, vol. 15, pp. 1217–1218.

[4] D. Farina, E. Schulte, R. Merletti, G. Rau, and C. Disselhorst-Klug, "Single motor unit analysis from spatially filtered surface electromyogram signals. Part I: Spatial selectivity," *Med. Biol. Eng. Comput.*, vol. 41, no. 3, pp. 330–337, 2003.

[5] M. M. Lowery, N. S. Stoykov, and T. A. Kuiken, "Independence of myoelectric control signals examined using a surface EMG model," *IEEE Trans. Biomed. Eng.*, vol. 50, no. 6, pp. 789–793, Jun. 2003.

[6] R. Rieger, "Variable-gain, low-noise amplification for sampling front ends," *IEEE Trans. Biomed. Circuits Syst.*, vol. 5, no. 3, pp. 253–261, Jun. 2011.

[7] J. Van Vugt and J. Van Dijk, "A convenient method to reduce crosstalk in surface EMG," *Clin. Neurophysiol.*, vol. 112, no. 2000, pp. 583–592, 2001.

[8] L. Christova, D. Stephanova, and A. Kossev, "Branched EMG electrodes for stable and selective recording of single motor unit potentials in humans," *Biomedizinische Technik/Biomedical Eng.*, vol. 52, no. 1, pp. 117–21, Feb. 2007.

[9] C. De Luca, R. Le Fever, and F. Stulen, "Pasteless electrode for clinical use," *Med. Biol. Eng. Comput.*, vol. 17, no. 3, pp. 387–390, 1979.

[10] X. Jiawei, R. Yazicioglu, B. Grundlehner, P. Harpe, K. A. Makinwa, and C. Van Hoof, "A 160 μW 8-channel active electrode system for EEG monitoring," *IEEE Trans. Biomed. Circuits Syst.*, vol. 5, no. 6, pp. 555–567, Dec. 2011.

[11] S. Nishimura, Y. Tomita, and T. Horiuchi, "Clinical application of an active electrode using an operational amplifier," *IEEE Trans. Biomed. Eng.*, vol. 39, no. 10, pp. 1096–1099, 1992.

[12] A. Searle and L. Kirkup, "A direct comparison of wet, dry and insulating bioelectric recording electrodes," *Phys. Meas.*, vol. 21, no. 2, pp. 271–283, 2000.

[13] J. C. Huhta and J. G. Webster, "60-HZ interference in electrocardiography," *IEEE Trans. Biomed. Eng.*, vol. BME-20, no. 2, pp. 91–101, Mar. 1973.

[14] A. C. M. van Rijn, A. Peper, and C. A. Grimbergen, "High-quality recording of bioelectric events: Part 1 interference reduction, theory and practice," *Med. Biol. Eng. Comput.*, vol. 28, no. 5, pp. 389–397, Sep. 1990.

[15] S. Johnson, P. Lynn, J. Miller, and G. Reed, "Miniature skin mounted preamplifier for measurement of surface electromyographic potentials," *Med. Biol. Eng. Comput.*, vol. 15, no. 6, pp. 710–711, 1977.

[16] S. Roy, G. De Luca, M. Cheng, A. Johansson, L. Gilmore, and C. De Luca, "Electro-mechanical stability of surface EMG sensors," *Med. Biol. Eng. Comput.*, vol. 45, no. 5, pp. 447–457, May 2007.

[17] F. N. Guerrero and E. Spinelli, "Surface EMG multichannel measurements using active, dry branched electrodes," in *Proc. IFMBE*, 2015, vol. 49, pp. 1–4.

[18] H. Broman, G. Bilotto, and C. De Luca, "A note on the noninvasive estimation of muscle fiber conduction velocity," *IEEE Trans. Biomed. Eng.*, vol. BME-32, no. 5, pp. 341–344, May 1985.

[19] H. Reucher, J. Silny, and G. Rau, "Spatial filtering of noninvasive multielectrode EMG: Part II-filter performance in theory and modeling," *IEEE Trans. Biomed. Eng.*, vol. BME-34, no. 2, pp. 106–113, Feb. 1987.

[20] G. V. Dimitrov, C. Disselhorst-Klug, N. A. Dimitrova, E. Schulte, and G. Rau, "Simulation analysis of the ability of different types of multielectrodes to increase selectivity of detection and to reduce cross-talk," *J. Electromyogr. Kinesiol.*, vol. 13, no. 2, pp. 125–138, Apr. 2003.

[21] T. Morrison, M. Nagaraju, B. Winslow, A. Bernard, and B. Otis, "A 0.5 CM3 four-channel 1.1 mW wireless biosignal interface with 20 m range," *IEEE Trans. Biomed. Circuits Syst.*, vol. 8, no. 1, pp. 138–147, Feb. 2014.

[22] T.-Y. Wang, M. R. Lai, C. M. Twigg, and S. Y. Peng, "A fully reconfigurable low-noise biopotential sensing amplifier with 1.96 noise efficiency factor," *IEEE Trans. Biomed. Circuits Syst.*, vol. 8, no. 3, pp. 411–422, Jun. 2014.

[23] Y. Li, A. Mansano, Y. Yuan, D. Zhao, and W. Serdijn, "An ECG recording front-end with continuous-time level-crossing sampling," *IEEE Trans. Biomed. Circuits Syst.*, vol. 8, no. 5, pp. 626–635, Oct. 2014.

[24] E. M. Spinelli, G. Hornero, O. Casas, and M. Haberman, "A design method for active high-CMRR fully-differential circuits," *Int. J. Instrum. Technol.*, vol. 1, no. 2, pp. 103–113, Jan. 2012.

[25] B. B. Winter and J. G. Webster, "Driven-right-leg circuit design," *IEEE Trans. Biomed. Eng.*, vol. BME-30, no. 1, pp. 62–6, Jan. 1983.

[26] A. Nonclercq and P. Mathys, "Reduction of power line interference using active electrodes and a driven-right-leg circuit in electroencephalographic recording with a minimum number of electrodes," in *Proc. 26th IEEE Ann. Int. Conf. Eng. Med. Biol. Soc. (EMBS)*, Sep. 2004, vol. 1, pp. 2247–2250.

[27] L. Geddes and M. Valentinuzzi, "Temporal changes in electrode impedance while recording the electrocardiogram with "dry" electrodes," *Ann. Biomed. Eng.*, vol. 1, no. 3, pp. 356–367, 1973.

[28] C. DeLuca, "The use of surface electromyography in biomechanics," *J. Appl. Biomech.*, vol. 13, no. 2, pp. 135–163, 1997.

[29] C. J. De Luca, M. Kuznetsov, L. D. Gilmore, and S. H. Roy, "Inter-electrode spacing of surface EMG sensors: Reduction of crosstalk contamination during voluntary contractions," *J. Biomechanics*, vol. 45, no. 3, pp. 555–61, Feb. 2012.

[30] E. Spinelli, N. H. Martinez, and M. A. Mayosky, "A single supply biopotential amplifier," *Med. Eng. Phys.*, vol. 23, no. 3, pp. 235–8, Apr. 2001.

Federico Nicolás Guerrero (S'13) was born in Comodoro Rivadavia, Argentina, in 1986. He received the Engineer degree in electronics from La Plata National University (UNLP), La Plata, Argentina, in 2011.

Since 2012, he has been working toward the Ph.D. degree at the Institute of Industrial Electronics, Control and Instrumentation (LEICI), UNLP and CONICET, La Plata, Argentina. He is also a Teaching Assistant in the UNLP Engineering Department. His research has been concerned with instrumentation and control for biopotential measurement systems.

Enrique Mario Spinelli was born in Balcarce, Argentina, in 1964. He received the Engineer degree in electronics and the M.S. and Ph.D. degrees from La Plata National University (UNLP), La Plata, Argentina, in 1989, 2000, and 2005, respectively.

Since 1990, he has been with the Institute of Industrial Electronics, Control and Instrumentation (LEICI), UNLP, and CONICET, La Plata, Argentina, where he is currently a Professor of control systems in the Engineering Department, working on scientific instrumentation. He is also a Researcher with the National Scientific and Technical Research Council (CONICET), Buenos Aires, Argentina. His research interests are analog signal processing and brain control interfaces.

Marcelo Alejandro Haberman was born in La Plata, Argentina, in 1984. He received the Engineer degree in electronics from La Plata National University (UNLP), La Plata, Argentina, in 2008.

Since 2008, he has been with the Institute of Industrial Electronics, Control and Instrumentation (LEICI), UNLP and CONICET, La Plata, Argentina, working on biopotential instrumentation. Currently, he is a Teaching Assistant in the Engineering Department at UNLP. His research interests are electronic instrumentation and human-computer interfaces.